Inorganic Chemistry
Article

Inorg. Chem. **2010**, *49*, 5063–5071 **5063**
DOI: 10.1021/ic100181d

Thermodynamic and Kinetic Control on the Formation of Two Novel Metal-Organic Frameworks Based on the Er(III) Ion and the Asymmetric Dimethylsuccinate Ligand

María C. Bernini,[†,‡] Victor A. de la Peña-O'Shea,[§] Marta Iglesias,[†] Natalia Snejko,[†] Enrique Gutierrez-Puebla,[†] Elena V. Brusau,[‡] Griselda E. Narda,[‡] Francesc Illas,[∥] and M. Ángeles Monge*[,†]

[†]*Instituto de Ciencia de Materiales de Madrid, CSIC, Madrid, Spain,* [‡]*Area de Química General e Inorgánica "Dr. G.F. Puelles", Facultad de Química, Bioquímica y Farmacia, Chacabuco y Pedernera, Universidad Nacional de San Luis, 5700 San Luis, Argentina,* [§]*Instituto Madrileño de Estudios Avanzados en Energía (IMDEA Energía), Universidad Rey Juan Carlos, Campus de Móstoles, Centro de Apoyo Tecnológico, C/Tulipán s/n E-28933 Móstoles, Madrid, Spain, and* [∥]*Departament de Química Física & IQTCUB, Universidad de Barcelona, Barcelona, Spain*

Received January 29, 2010

Two new layered polymeric frameworks have been synthesized under different hydrothermal conditions and characterized by single-crystal X-ray diffraction, thermal analysis, and variable temperature-Fourier Transform Infrared Spectroscopy (VT-FTIR). The compound I, with formula $[Er_2(dms)_3(H_2O)_4]$, has a triclinic cell with parameters a=5.8506 Å, b=9.8019 Å, c=11.9747 Å, α=70.145°, β=80.234°, and γ=89.715°, and the compound II, $[Er_2(dms)_3(H_2O)]$, is monoclinic and its cell parameters are a=11.1794 Å, b=18.2208 Å, c=12.7944 Å, β=112.4270°, where dms=2,2-dimethylsuccinate ligand. A theoretical study including energy calculations of the dms conformers was carried out at the Density Functional Theory (DFT-B3LYP) level of theory, using the 6-311G* basis set. Further calculations of the apparent formation energies of I and II crystalline structures were performed by means of the periodic density functional theory, using DF plane-waves. The analysis of the structural features, theoretical relative stabilities, and the influence of synthesis conditions are presented here. The heterogeneous catalytic activity of the new compounds is tested and reported.

Introduction

Attracted by the special chemical and physical properties of lanthanide elements, as well as by their compounds' intriguing structural motifs and potential applications in selective catalysis, gas storage, luminescence, magnetism, spin-transition (spin-crossover), nonlinear optics (NLO), and so forth[1], many efforts have been made to synthesize novel lanthanide Metal-Organic Frameworks (MOFs). A wide combination of simple organic linkers, like succinate, with rare earth ions led to both a rich variation and modulation of open-framework structures and physical properties of the resultant solid materials.[2]

As is well known, the synthesis conditions are very important to obtain a certain compound; pH value, solvent type, time and temperature of reaction are the most important factors susceptible to change for the rational design of MOFs.[3,4] The variation of temperature and time of reaction allows us to investigate the existence of a thermodynamic or kinetic control on the formation of a specific phase. This aspect has been widely studied in the organic synthesis field: new synthetic protocols have been developed, operating under both kinetic and thermodynamic control, for the

*To whom correspondence should be addressed. E-mail: amonge@icmm.csic.es.

(1) (a) Janiak, C. *Dalton Trans.* **2003**, 2781. (b) Mueller, U.; Schubert, M.; Teich, F.; Puetter, H.; Schierle-Arndt, K.; Pastré, J. *J. Mater. Chem.* **2006**, *16*, 626.

(2) (a) Seguatni, A.; Fakhfakh, M.; Vauley, M. J.; Jouini, N. *J. Solid State Chem.* **2004**, *177*, 3402. (b) Perles, J.; Iglesias, M.; Ruiz Valero, C.; Snejko, N. *J. Mater. Chem.* **2004**, *14*, 2683. (c) Bernini, M. C.; Brusau, E. V.; Narda, G. E.; Echeverría, G. E.; Pozzi, C. G.; Punte, G.; Lehmann, C. W. *Eur. J. Inorg. Chem.* **2007**, *5*, 684. (d) Serpaggi, F.; Ferey, G. *Microporous Mesoporous Mater.* **1999**, *32*, 311. (e) Fleck, M. Z. *Kristallogr. NCS* **2002**, *217*, 569.

(3) (a) Forster, P. M.; Burbank, A. R.; Livage, C.; Ferey, G.; Cheetham, A. K. *Chem.Commun.* **2004**, 368. (b) Forster, P. M.; Stock, N.; Cheetham, A. K. *Angew. Chem., Int. Ed.* **2005**, *44*, 7608. (c) Forster, P. M.; Burbank, A. R.; O'Sullivan, M. C.; Guillou, N.; Livage, C.; Ferey, G.; Stock, N.; Cheetham, A. K. *Solid State Sci.* **2005**, *7*, 1549. (d) Livage, C.; Egger, C.; Ferey, G. *Chem. Mater.* **2001**, *13*, 410.

(4) (a) Harvey, H. G.; Slater, B.; Attfield, M. P. *Chem.−Eur. J.* **2004**, *10*, 3270. (b) Lee, C.; Mellot-Draznieks, C.; Slater, B.; Wu, W. G.; Harrison, T. A.; Rao, C. N. R.; Cheetham, A. K. *Chem. Commun.* **2006**, 2687.

Published on Web 04/29/2010

preparation of stable phases;[5] numerous examples exist that reflect the influence of reaction conditions on the formation of a specific product.[6] In the case of MOFs, however, few combined experimental and computational studies have been performed to study this matter,[4b,7] and thus, further research is needed.

Rare earths succinates have been profusely investigated, and several structures employing this ligand have been obtained and characterized.[2] In particular, with Er(III) ion a number of succinate compounds have been reported.[8] However, MOFs based on substituted succinates ligands, like alkyl- and aryl-succinates, have not been largely explored yet.[9]

Continuing our research on rare earth MOFs, this paper is addressed toward the use of the acentric substituted succinate ligand, namely, 2,2-dimethylsuccinic acid. This is a flexible and versatile ligand for the construction of coordination polymers; its two carboxylate groups may be completely or partially deprotonated, resulting in many coordination modes and formation of the lanthanide clusters, which may act as secondary building units to construct frameworks with novel structural features. Besides, as it has been demonstrated recently, the flexibility of the ligand is a key factor in the structure development, being associated not only with the possibility of existence of interpenetration of the networks[10] and its degree and mode of interpenetration[11] but also with the need to fit the coordination environment of a metal ion.[12] In turn, the frequency for a conformationally flexible molecule with no-chiral center to crystallize in a non-centrosymmetric group is higher than that for the molecules categorized as rigid with no-chiral center.[13] Being a current emerging trend, the preparation of non-centrosymmetric solids has not been profusely investigated, and not many MOFs based on asymmetric substituted succinate ligands have been explored yet. That is why it seems interesting to study the possibility of getting both centrosymmetric and acentric frameworks by tuning thermodynamically or kinetically the synthesis conditions.

Here we report the synthesis, crystal structures, and characterization of two different frameworks based on erbium(III) ion and 2,2-dimethylsuccinate ligand: a chiral 2D-layered MOF and a centrosymmetric 2D-mixed organic−inorganic layered MOF obtained under different hydrothermal conditions. An appropriate combination of experimental and computational studies was performed to shed light on the mechanism of formation of these MOFs. The activity of both compounds as redox catalysts has been evaluated in the oxidation of methylphenylsulfide.

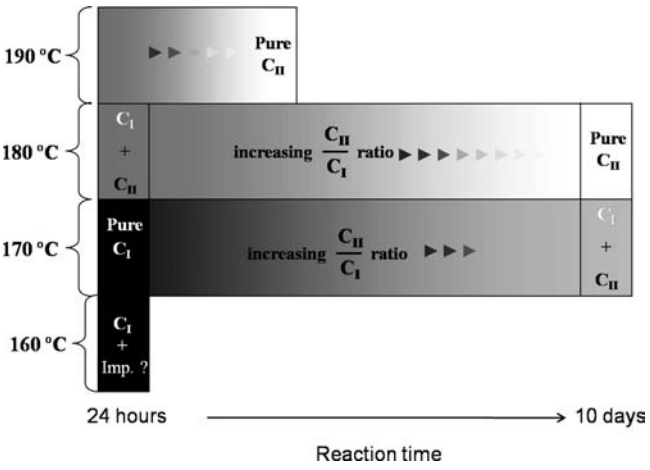

Figure 1. Phase diagram scheme.

Experimental Section

General Synthesis Procedure. All reagents were purchased at high purity (AR grade) from Aldrich (2,2-dimethylsuccinic acid) and Strem Chemicals [$Er(NO_3)_3 \cdot 5H_2O$] and were used without further purification.

Both compounds were obtained by hydrothermal reaction of 1 mmol of $Er(NO_3)_3 \cdot 5H_2O$ with 1.5 mmol of the ligand ($C_6H_{10}O_4$ = H_2dms) in 10 mL of water. The final pH value was adjusted to 4.5 with 0.1 mL of pyridine. For [$\mathbf{Er_2(dms)_3(H_2O)_4}$] (**I**), the mixture was put in a Teflon-lined digestion bomb (internal volume of 43 mL), at 170 °C during 24 h and then cooled to room temperature. Pink prismatic crystals were collected after washing with distilled water and acetone (yield 83.7%). [$\mathbf{Er_2(dms)_3(H_2O)}$] (**II**) was obtained following a similar procedure at 180 °C during 10 days (yield 26.8%) or 190 °C during 4 days (yield 72.2%). Pink prismatic hexagonal crystals were collected after washing with distilled water and acetone.

A compound I-enriched mixture of I and II is obtained after 24 h at 180 °C; increasing amounts of II appear during the progress of the reaction time to render pure compound II after 10 days. A similar situation occurs at 190 °C but the pure compound II is achieved in 4 days (see Figure 1).

Crystal Structure Determination. Single crystals of compounds I and II were mounted on a Bruker-Siemens Smart CCD diffractometer equipped with a normal focus, 2.4 kW sealed tube X-ray source (temperature = 296(2) K, MoK_α radiation, λ = 0.71073 Å) operating at 40 kV and 30 mA for compound I and 5 mA for compound II. Data were collected over a hemisphere of reciprocal space by a combination of three sets of exposures. Each set had a different θ angle for the crystal and each exposure of 10 s for both compounds covered 0.3° in ω. The crystal-to-detector distance was 5.5 cm. Coverage of the unique set was over 99% complete to at least 23° in θ. Unit cell dimensions were determined by a least-squares fit of reflections with $I > 2\sigma(I)$. A semiempirical absorption and scale correction based on equivalent reflection was carried out using SADABS.[14]

(5) Dichtel, W. R.; Miljanic, O.; Zhang, W.; Spruell, J. M.; Patel, K.; Aprahamian, I.; Heath, J. R.; Stoddart, J. F. *Acc. Chem. Res.* **2008**, *41*(12), 1750.

(6) (a) Carey, F. A.; Sundberg, R. J., *Advanced Organic Chemistry*, 3rd ed.; Plenum Press: New York, 1990. (b) Ruff, F.; Csizmadfia, I. G., Studies in Organic Chemistry. *Organic Reactions, Equilibria, Kinetic and Mechanism*; Elsevier: Amsterdam, 1994. (c) Rodriguez-Spong, B.; Price, Ch. P.; Jayasankar, A.; Matzger, A. J.; Rodriguez-Hornedo, N. *Adv. Drug Delivery Rev.* **2004**, *56*, 241.

(7) Gándara, F.; de la Peña O'Shea, V.; Illas, F.; Snejko, N.; Proserpio, D. M.; Gutierrez-Puebla, E.; Monge, M. A. *Inorg. Chem.* **2009**, *48*, 4707.

(8) (a) Li, H. *Acta Crystallogr., Sect. E: Struct. Reports Online* **2007**, *63*(3), 840. (b) Sun, J.; Zheng, Y.-Q.; Lin, J. L. *Z. Kristallogr.*: NCS 2004, *219*, 99. (c) Nika, W.; Pantenburg, I.; Meyer, G. *Acta Crystallogr., Sect. E.* **2005**, *61*, 138. (d) Dong, G.-Y.; Cui, G.-H.; Lin, J. *Acta Crystallogr., Sect. E: Struct. Reports Online* **2006**, *62*, m738. (e) He, Q.; Zi, J.-F.; Zhang, F.-J. *Acta Crystallogr., Sect. E: Struct. Reports Online* **2006**, *62*, m997.

(9) (a) Brown, K. A.; Martin, D. P.; Supkowski, R. M.; LaDuca, R. L. *CrystEngComm* **2008**, *10*, 846. (b) Lyons, E. M.; Braverman, M. A.; Supkowski, R. M.; LaDuca, R. L. *Inorg. Chem. Commun.* **2008**, *11*, 855. (c) Zhou, J.; Sun, C. Y.; Jin, L. P. *Polyhedron* **2007**, *26*, 4025. (d) Fischer, A. *Acta Crystallogr.* **2005**, *E61*, 320.

(10) Aakeröy, C. B.; Champness, N. R.; Janiak, C. *CrystEngComm* **2010**, *12*, 22.

(11) Yang, J.; Ma, J.-F.; Liu, Y.-Y.; Batten, S. R. *CrystEngComm* **2009**, *11*, 151.

(12) Yang, P. P.; Li, B.; Wang, Y. H.; Gu, W.; Liu., X. *Z. Anorg. Allg. Chem.* **2008**, *634*, 1210.

(13) Pidcock, E. *Chem. Commun.* **2005**, 3457.

(14) *SAINT, data collection and procedure software for the SMART system*; Siemens Analytical X-ray Instruments, Inc.: Madison, WI, 1995.

Table 1. Crystallographic Data for Compounds I and II

	compound I	compound I	compound II
formula	$[Er_2C_{18}H_{24}O_{16}]$	$[ErC_9H_{12}O_8]$	$[Er_2C_{18}H_{26}O_{13}]$
molecular weight/gmol^{-1}	838.96	418.47	784.91
crystal system	triclinic		monoclinic
space group	$P\bar{1}$	$P\bar{1}$	$P2_1/c$
a/Å	5.8506(6)	5.8506(6)	11.1794(5)
b/Å	9.8019(9)	9.8019(9)	18.2208(8)
c/Å	11.9747(11)	11.9747(11)	12.7944(6)
α/ deg	70.145	70.145	90.00
β/ deg	80.234(1)	80.234(1)	112.4270(10)
γ/ deg	89.715(1)	89.715(1)	90.00
V/Å^3	635.51(11)	635.51(11)	2409.07(19)
Z	1	2	4
calc. density/g cm^{-3}	2.192	2.187	2.164
μ/mm^{-1}	6.632	6.632	11.89
dimensions (mm)	0.2 × 0.15 × 0.08	0.2 × 0.15 × 0.08	0.15 × 0.15 × 0.05
limiting indices			
h		$-7 < h < 7$	$-13 < h < 13$
k		$-11 < k < 11$	$-21 < k < 21$
l		$-14 < l < 14$	$-15 < l < 15$
F(000)	404.0	402	1496
reflections collected/unique with $I > 2\sigma(I)$	3933/3585	2203/1727	4379/3635
refined parameters	331	158	304
Flack parameter (TWIN + BASF)/esd	0.501/0.011		
$\lvert E^2-1\rvert$[a]	0.649		
goodness-of-fit on F^2	1.054	1.009	0.985
R_1	0.0393	0.0616	0.0422
wR_2	0.0856	0.1220	0.0812

[a] Expected values: 0.968, for centrosymmetric; 0.736 for non-centrosymmetric.

Space group determinations were carried out using XPREP.[15] The structures were solved by direct methods and refined by anisotropic full-matrix least-squares, except for hydrogen atoms as a pseudo-centrosymmetric $P\bar{1}$ structure (compound I) or in the monoclinic space group (S.G.) $P2_1/c$ (compound II). A summary of the conditions for data collection and structure refinement is given in Table 1. For both compounds, the coordinated water hydrogen atoms were located. All calculations were performed using the following: SMART software for data collection; SAINT *plus* program[14] for integration and scale correction of data; SHELXTL[15] to resolve and refine the structure and to prepare material for publication; and ATOMS[16] for molecular graphics.

CCDC 763862−763864 contain the supplementary crystallographic data for this paper. These data can be obtained free of charge from The Cambridge Crystallographic Data Center via www.ccdc.cam.ac.uk/data_request/cif.

Characterization. The FTIR spectra were recorded on a Nicolet PROTÉGÉ 460 spectrometer provided with a CsI beamsplitter in the 4000−250 cm^{-1} range with 64 scans and spectral resolution of 4 cm^{-1}, using the KBr pellet technique. Variable Temperature Fourier Transform Infrared (VT-FTIR) spectra were recorded using an accesory developed by Seasing SRL (La Plata, Argentina) that consists in a variable-temperature IR cell provided with KBr windows operating under high vacuum. The temperature controller allows the cell to collect spectra between room temperature and 270 °C.

Thermogravimetric and differential thermal analyses (TGA/DTA) were performed using a SEIKO TG/DTA 320 apparatus in the temperature range 25−1000 °C in air atmosphere (flow of 100 mL/min) at a heating rate of 10 °C/min.

Catalytic Activity Test: Oxidation of Methylphenylsulfide. To find the most suitable operating conditions, a study of catalyst activation temperatures (T_a) and reaction temperatures (T_r) was performed: T_a = 60 °C and T_r = Room Temperature, T_a = 60 °C and T_r = 60 °C and finally T_a = 80 °C and T_r = 60 °C, keeping the time of activation of the catalyst always equal to 1 h. The last T_a and T_r mentioned were selected for the tests.

In this way, the catalysts (0.05 mmol based on Er ion) were activated by stirring with hydrogen peroxide (1.5 mmol, 25%) for 1 h at 80 °C in a 25 mL flask equipped with a magnetic stirrer. Later the system was cooled to 60 °C, and the reaction was carried out at this temperature. The reactor with the activated catalyst was then charged with acetonitrile (3 mL) and the corresponding thioether (methylphenylsulfide, 2.52 mmol), and H_2O_2 (1.5 mmol, 25%) was added dropwise. Samples were taken hourly and analyzed after filtration. Chemical yields of sulfoxides and sulfones were measured by gas chromatography (GC) on a Hewlett-Packard 5890 II chromatograph with a β-DEX325 capillary column, equipped with an MS detector.

Recycling Experiment. Compound I was reused in several methylphenylsulfide oxidation reaction cycles. Before reuse, the solid was filtered from the reaction medium and washed with diethyl ether; then fresh substrate, oxidant agent, and solvent were added without additional amount of catalyst, in three consecutive experiments. To verify the heterogeneous nature of the catalytic reaction, the residual activity of the supernatant solution after separation of the catalyst was studied. To rule out a potential leaching, the liquid phase of the first run was separated from the solid (catalyst). New fractions of reagents were added to the clear filtrate, and the composition of the homogeneous reaction mixture was determined by GC. This mixture was used in a standard catalytic experiment. After 5 h the mixed composition was checked, and no reaction was observed, which excluded the presence of active catalytic species in solution.

Computational Details. The structural energy calculations on the 2,2-dms conformers were made using the density functional theory (DFT) with the hybrid Becke three-parameters exchange functional (B3)[17] in combination with the Lee−Yang−Parr correlation functional (B3LYP).[18] The standard split-valence

(15) *SHELXTL*, version 5.0; Siemens Analytical X-ray Instruments, Inc.: Madison, WI, 1995.

(16) Dowty, E. *ATOMS for Windows , a computer program for displaying atomic structure*, Version 3.1; Shape Software: Kingsport, TN, 1995.

(17) Becke, A. D. *J. Chem. Phys.* **1993**, *98*, 5648.

(18) Lee, C.; Yang, W.; Parr, R. G. *Phys. Rev. B* **1988**, *37*, 785.

basis set used was 6-311G*. All calculations were performed using the Gaussian 03 set of programs.[19] The structural energy calculations were done employing fixed values for the dihedral angles C−C−C−C, O−C−C−C, and C−C−C−O depending on the conformation of each dms ligand present in both structures.

The structural stability ab initio calculations on compounds I and II have been carried out by means of the periodic density functional theory. The DF plane-wave calculations were realized using the VASP package,[20,21] considering spin-polarization and dipole corrections explicitly. The total energy was computed using the revised Perdew−Burke−Ernzerhof GGA (RP)[22,23] exchange-correlation function, via the spin-interpolation formula of Vosko−Wilk−Nusair (VWN).[24,25] The effect of the core electrons on the valence electron density was described by the projector augmented wave (PAW) method.[26,27] The cutoff for the kinetic energy of the plane-waves has been set to 415 eV throughout, which after extensive test proved to ensure a total energy convergence better than 10^{-4} eV. A Gaussian smearing technique with a 0.1 eV width has been applied to enhance convergence, but all energies presented here have been obtained by extrapolating to zero smearing (0K). Integration in the reciprocal space was achieved using the Monkhorst−Pack method[28] with three k-points in the Brillouin zone. The convergence with respect to the number of k-points was better than that of the cutoff energy. Geometry optimization on selected starting geometries obtained from single crystal X-ray diffraction was carried out using a gradient-conjugate method until forces on all atoms were less than 0.3 eV/nm. The apparent formation energy was calculated as an energy difference between the corresponding reagents and MOFs products. All calculations were performed on a parallel CESCA supercomputer.[29]

Results and Discussion

Effects of Synthesis Conditions. To isolate both compounds as pure phases, several synthetic experiments on the system Er-dms-H_2O were carried out. Once the stoichiometric amounts of reactants were fixed, the effect of temperature and time variation was studied with the following results.

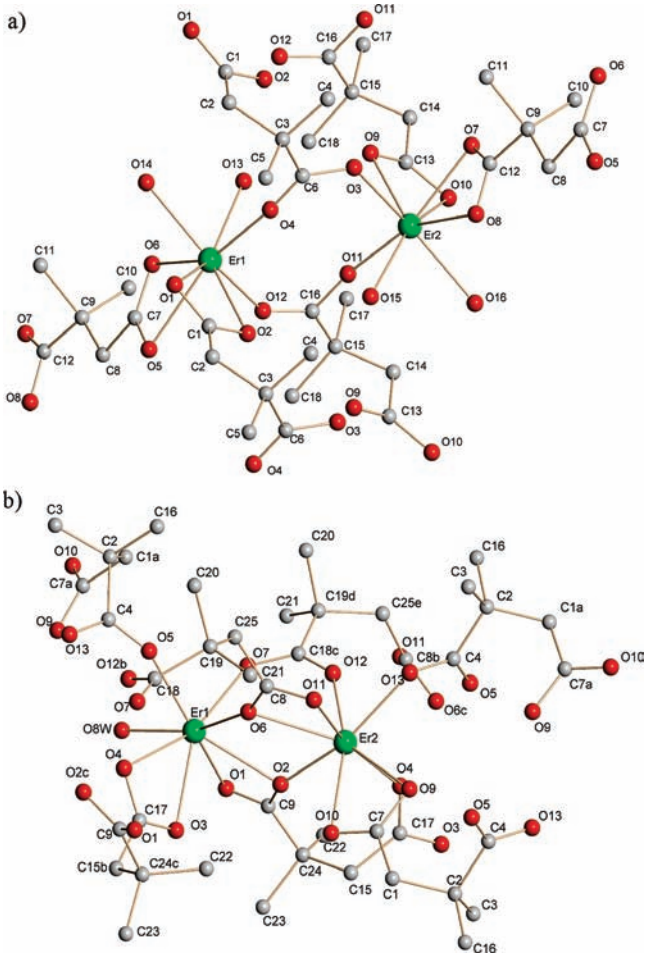

Figure 2. Coordination environments of (a) $[Er_2(dms)_3(H_2O)_4]$ (I) and (b) $[Er_2(dms)_3(H_2O)]$ (II). Symmetry Operations for equivalent atoms. **a**: $-x+1, -y, -z$; **b**: $x, -y+1/2, z+1/2$; **c**: $x, -y+1/2, z-1/2$; **d**: $x, y, z-1$; **e**: $x, y, z+1$.

Compound I is obtained at 170 °C in 24 h as a pure phase, and some traces of compound II appears in about 8 days. If the temperature drops to 160 °C, in 1 day the compound I is obtained with a small amount of an unknown impurity, but no trace of compound II appears at this temperature. When trying to obtain compound II by increasing the temperature at 180 °C, a mix of the 2 phases is obtained depending on the time of reaction. At this temperature a mixture of I with a small amount of II also appears in 1 day, but the amount of II increases in such a way that in 4 days 50% of each phase is obtained, and then the compound II proportion increases up to 100% in 10 days. In turn, if the temperature rises to 190 °C, only 4 days are sufficient to obtain the compound II as a single phase. The Figure 1 is a schematic representation of the synthesis conditions study.

Structural Description. $[Er_2(dms)_3(H_2O)_4]$ (I). Although the structure is non-centrosymmetric and has been solved and isotropically refined in the triclinic $P1$ space group (S.G.), the existence of strong correlations in the anisotropic refinement matrix forces to refine anisotropically the structure as pseudocentrosymmetric in the $P\bar{1}$ S.G., giving occupation factors $=1/2$ to the methyl groups of the *trans* dms anion. To rule out the centrosymmetric space group and the existence of a non resolvable

(19) Frisch, M. J., Trucks, G. W., Schlegel, H. B., Scuseria, G. E., Robb, M. A., Cheeseman, J. R., Montgomery, J. A., Vreven, Jr., T., Kudin, K. N., Burant, J. C., Millam, J. M., Iyengar, S. S., Tomasi, J., Barone, V., Mennucci, B., Cossi, M., Scalmani, G., Rega, N., Petersson, G. A., Nakatsuji, H., Hada, M., Ehara, M., Toyota, K., Fukuda, R., Hasegawa, J., Ishida, M., Nakajima, T., Honda, Y., Kitao, O., Nakai, H., Klene, M., Li, X., Knox, J. E., Hratchian, H. P., Cross, J. B., Adamo, C., Jaramillo, J., Gomperts, R., Stratmann, R. E., Yazyev, O., Austin, A. J., Cammi, R., Pomelli, C., Ochterski, J. W., Ayala, P. Y., Morokuma, K., Voth, G. A., Salvador, P., Dannenberg, J. J., Zakrzewski, V. G., Dapprich, S., Daniels, A. D., Strain, M. C., Farkas, O., Malick, D. K., Rabuck, A. D., Raghavachari, K., Foresman, J. B., Ortiz, J. V., Cui, Q., Baboul, A. G., Clifford, S., Cioslowski, J., Stefanov, B. B., Liu, G., Liashenko, A., Piskorz, P., Komaromi, I., Martin, R. L., Fox, D. J., Keith, T., Al-Laham, M. A., Peng, C. Y., Nanayakkara, A., Challacombe, M., Gill, P. M. W., Johnson, B., Chen, W., Wong, M. W., Gonzalez, C., Pople, J. A. *Gaussian 03*, Revision B.01; Gaussian, Inc.: Pittsburgh, PA, 2003.
(20) Kresse, G.; Furthmüller, J. *Comput. Mater. Sci.* **1996**, *6*, 15.
(21) Kresse, G.; Hafner, J. *Phys. Rev. B* **1993**, *47*, 558.
(22) Perdew, J. P.; Wang, Y. *Phys. Rev. B* **1992**, *45*, 13244.
(23) Perdew, J. P.; Chevary, J. A.; Vosko, S. H.; Jackson, K. A.; Pederson, M. R.; Singh, D. J.; Fiolhais, C. *Phys. Rev. B* **1992**, *46*, 6671.
(24) Zhang, Y.; Yang, W. *Phys. Rev. Lett.* **1998**, *80*, 890.
(25) Vosko, S. H.; Wilk, L.; Nusair, M. *Can. J. Phys.* **1980**, *58*, 1200.
(26) Blöchl, P. E. *Phys. Rev. B* **1994**, *50*, 17953.
(27) Kresse, G.; Joubert, D. *Phys Rev B* **1999**, *59*, 1758.
(28) Monkhorst, H. J.; Pack, J. D. *Phys. Rev. B* **1976**, *13*, 5188.
(29) For details about the supercomputer architecture see: www.cesca.es.

Table 2. Selected Bond Distances of Compound I and Compound II

bond	distance (Å)	bond	distance (Å)
	Compound I		
Er1−O1	2.426(3)	Er2−O7	2.388(2)
Er1−O2	2.400(2)	Er2−O8	2.412(2)
Er2−O3	2.354(2)	Er2−O9	2.380(2)
Er1−O4	2.244(2)	Er2−O10	2.413(3)
Er1−O5	2.546(2)	Er2−O11	2.225(2)
Er1−O6	2.341(2)	Er2−O12	2.211(3)
Er1−O13w	2.412(2)	Er2−O15w	2.327(2)
Er1−O14w	2.328(2)	Er2−O16w	2.353(2)
	Compound II		
Er1−O1	2.411(4)	Er2−O2	2.311(4)
Er1−O2	2.411(4)	Er2−O4	2.289(4)
Er1−O3	2.396(5)	Er2−O6	2.501(4)
Er1−O4	2.451(4)	Er2−O9	2.382(4)
Er1−O5	2.221(5)	Er2−O10	2.367(5)
Er1−O6	2.322(4)	Er2−O11	2.399(4)
Er1−O7	2.269(5)	Er2−O12	2.270(5)
Er1−O8w	2.299(4)	Er2−O13	2.292(5)

positional disorder, we carried out the resolution of the structure in the *P*1 space group, where we found that the occupation factors of the methyl groups of the *trans* dms anion were equal to 1. If such disorder would exists, the occupation factors of these methyl groups should have been 1/2 also in the *P*1 space group. Furthermore, no residual electron density was found around the C8 atom while using the Fourier method in the refinement process, which indicates that the chosen *P*1 space group is the most appropriate for the structure under consideration. These methyl groups are the only ones that break the symmetry of the inversion center. A description based on *P*1 S.G. is given here.

In the asymmetric unit there are two independent Er(III) ions surrounded by three independent dms anions. One of them has a *trans* conformation with a torsion angle (C1C2C3C4) = −173.3°, whereas the other ones have different torsion angles (C1C2C3C4) in a *gauche* conformation: −43.1° ($dmsA^I$) and 61.5° ($dmsB^I$) (Figure 2 left). Both Er ions are coordinated to eight oxygen atoms, six of which belong to carboxylate groups and two to coordinated water molecules, giving rise to triangulated dodecahedra. Er−O bond lengths lie in the range 2.211(3)−2.546(2) Å, which is consistent with that of previously reported erbium succinates frameworks[8a,b] (See Table 2).

The ErO_8 polyhedra are linked in the [0 1 −1] direction by the *trans* dms conformer, whereas $dmsA^I$ and $dmsB^I$ connect polyhedra in the [1 0 0] direction (Figure 3 left). The *trans* dms anion acts in η^2– η^2 chelate mode by its two carboxylate groups; the distance between the α and ω carbon atoms is 3.906(4) Å. The $dmsA^I$ and $dmsB^I$ ligands act both in a η^2 chelate mode by one carboxylate group and as $\eta^2\mu_2$ bidentate by the other one, the distance between α and ω carbon atoms being 2.996(5) Å and 3.034(5) Å for $dmsA^I$ and $dmsB^I$, respectively (Figure 4 up).

The resultant 2D hybrid framework belongs to the I^0O^2 type[4b] (Figure 3 left) with layers that extend parallel to the *ac* plane.

The hydrogen bonds found in the framework strengthen the structure. The water molecules W14 and W16 are

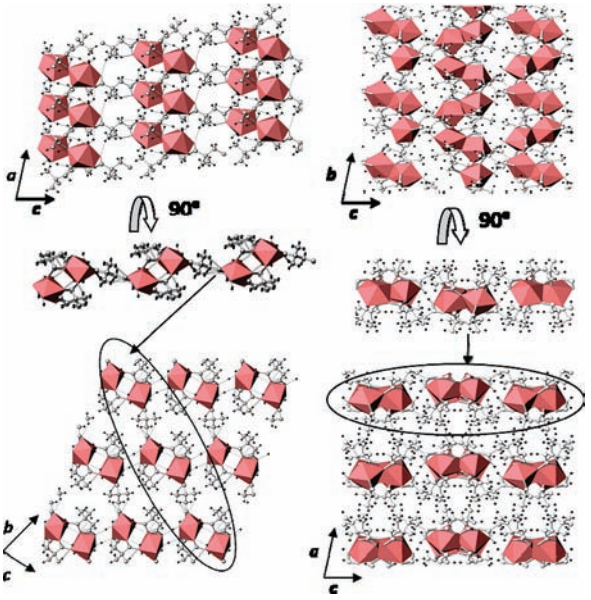

Figure 3. Structure of (left)(I), and (right) (II) showing the layers and their direction in the framework.

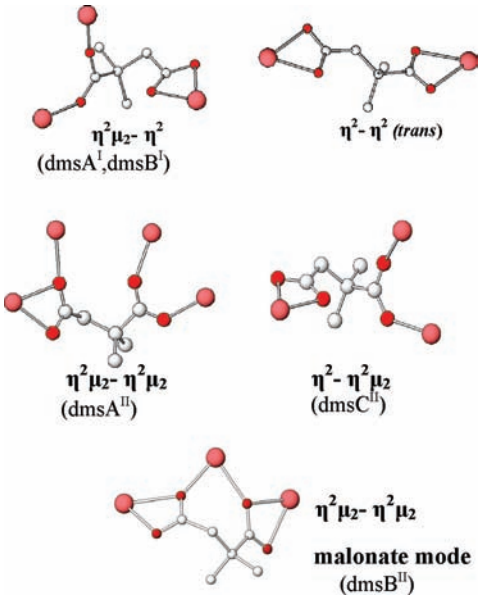

Figure 4. Representation of dms coordination modes for (up) compound I, and (down) compound II.

involved in two interactions as H-donor: one of them is inside the layer, bonding both carboxylate groups of the *trans* dms ligand through O5 and O7, respectively, and the remaining interaction is between layers involving O10 and O1, respectively. The water molecule W13 acts as H-donor to O5 whereas W15 is involved in two interactions of the same type to O2 and O3 atoms. It is remarkable that the interactions that take place between layers involving W14 and W16 are the strongest of all those that compose the H-bond net.

There are two geometrical features in compound I that explain the lack of inversion center in the triclinic cell: the gem-dimethyl substitution on the *trans* dms ligand, and the strong inductive effect in this ligand that causes the decrease of the closer O−C bond distances (see the

corresponding cif file). On the other hand, the diminution of symmetry that suffers the *trans* dms linker, when it is incorporated in the crystal, is manifested in the twisted conformation (dihedral angle CCCC = −173.3°) that it acquires. If the structure is refined in the $P\bar{1}$ space group, the mentioned dihedral angle is forced to adopt the value of 180° and the C−O bond distances of the *trans* dms anion are not different, thus eliminating the inductive effect exerted by the methyl groups in this conformer. Such model causes tension in the structure reflected in the worst R1 and wR2 index values (0.0616 and 0.1220, respectively) whereas the refinement in P1 leads to a more relaxed structure. This is confirmed by the better values of such indexes (0.0393 and 0.0856) even having the double number of refined parameters than in the $P\bar{1}$ space group.

[Er_2(dms)$_3$(H_2O)] (II). This compound crystallizes in the monoclinic $P2_1/c$ S.G. In the asymmetric unit there are two Er ions with the same coordination number (eight) but different coordination environments. The Er1 ion is surrounded by seven oxygen atoms from carboxylate groups and one oxygen atom from a coordinated water molecule. All oxygen atoms of the Er2 coordination sphere belong to carboxylate groups (Figure 2 right). The coordination polyhedra of both metal centers are, as in compound I, triangulated dodecahedra.

The Er1−O bond lengths fall in the range 2.221(5)−2.451(4) Å whereas the Er2−O ones are in the range 2.270(5)−2.501(4) Å.

The SBU (secondary building unit) in II consists of chains of alternatively sharing vertex and edges polyhedra running in zigzag mode along the *c* direction. As a consequence, the distances between adjacent metal centers inside the chain are not equivalent. The Er···Er distance for the edge-sharing polyhedra is 3.857 Å, whereas polyhedra linked by a vertex are separated for 4.304 Å. The chains are connected in the *b* and *c* directions by three dms anions in three non-equivalent *gauche* conformations, as it can be seen in Figure 3, down.

It has been shown that the more elevated the synthesis temperature is, the higher the amount of *gauche* conformer ligands surround the cation.[30] In our case, we go from compound I, in which there are two *gauche* and one *trans* conformer, to compound II, in which no trans isomer appears, by raising the synthesis temperature 10 degrees and augmenting the time of reaction (Figure 1).

The dms anion that extends in the *c* direction (dmsA^{II}) has a torsion angle (C1C2C3C4) of −64.97° and a distance between α and ω carbon atoms of 3.048(9) Å. One of the carboxylate groups of this anion coordinates through a chelate-bridge interaction while the other one acts as bidentate-bridge; thus, this ligand $\eta^2\mu_2$-$\eta^2\mu_2$ connects four consecutively erbium ions of the SBU. Another dms ligand (dmsB^{II}) bears a V-shape, with a (C1C2C3C4) dihedral angle of 77.62°, and has a distance between α and ω carbon atoms of 3.238(9) Å. This dmsB^{II} ligand links three consecutive erbium ions of the chain in a double chelate-bridge fashion, where the central Er cation is bonded to its two carboxylate groups. As a result, a seven-membered ring is formed. This particular way of coordination (Figure 4 down), named "*malonate mode*",[31] present in several metal malonates, is unusual in longer aliphatic dicarboxylates. It has been reported for a glutarate of lanthanum[32] and to our knowledge it is the first example in succinate MOFs.

The third dms anion (dmsC^{II}) links the polyhedra in the *b* direction, and has a torsion angle (C1C2C3C4) of −82.33°, the distance between the α and ω carbon atoms being 3.337(9) Å. This ligand (dmsC^{II}) acts as a η^2–$\eta^2\mu_2$ linker placed between the inorganic chains, chelating one erbium ion by one carboxylic extreme and in a bidentate-bridge mode by the other one, linking two erbium ions from a chain. This connection is reinforced by two H-bond interactions between the H-donor coordination water molecule and two O atoms belonging to different carboxylate groups in the neighboring chain.

The chain of polyhedra, constructed by **c** glide plane (x, $1/2-y$, $1/2+z$) runs parallel to the *c* axis, with participation of the dmsA^{II} and dms B^{II} ligands.

The resultant framework is bidimensional and corresponds to the I^1O^1 type[4b] with layers extending parallel to the *bc* plane (see Figure 3, right).

Contrary to the compound I, no H-bonds between layers are observed in this framework, and the stabilization is achieved by London interactions in the *a* direction that favors the network packing.

Computational Study. Conformational and energetic DFT calculations are commonly used in several chemistry fields like organic and inorganic small molecules based-systems. In the case of MOF materials, the large number of atoms that may contain this type of compounds combined with the presence of heavy metal ions such as rare earth ones, makes this process more complicated, and the use of this theoretical calculation methodology is not common yet.[7,33] However, theoretical calculations, as a complement in the determination of the factors that govern the mechanisms of formation of MOFs, are quite useful.

As a first approximation, structural energy calculations of the different conformations adopted by the dms ligand in compounds I and II were made at the DFT B3LYP-6311G* level of theory, employing the Gaussian 03 set of programs[19] (see Computational Details). The obtained results show a total stabilization (of ∼22 kcal/mol) for the conformations corresponding to the compound II (Figure 5, Supporting Information, Table S1).

To determine the structural stability of these compounds and to deepen the understanding of their formation pathways, a series of theoretical DF plane-wave based calculations were carried out. The apparent energies of formation were obtained using the VASP package[20,21] (see Computational Details). The geometry optimization converged to a stable structure with the same topology that the experimental structures obtained

(30) Bernini, M. C.; Brusau, E. V.; Narda, G. E.; Echeverría, G. E.; Pozzi, C. G.; Punte, G.; Lehmann, C. W. *Eur. J. Inorg. Chem.* **2007**, *5*, 684.

(31) (a) Farago, M. E.; Amirhaeri, S. *Inorg. Chim. Acta* **1984**, *81*, 205. (b) Karipides, A.; Ault, J.; Reed, A. T. *Inorg. Chem.* **1977**, *16*, 3299. (c) Benmerad, B.; Guehria-Laïdoui, A.; Bernardinelli, G.; Balegroune, F. *Acta Crystallogr.* **2000**, *C56*, 321.

(32) Benmerad, B.; Guehria-Laïdoui; Dahaoudi, S.; Lecomte, C. *Acta Crystallogr.* **2004**, *C60*, m119.

(33) (a) Keskin, S.; Liu, J.; Rankin, R. V.; Karl Jhonson, J.; Sholl, D. S. *Ind. Eng. Chem. Res.* **2009**, *48*, 2355 and references therein. (b) Coombes, D. S.; Cora, F.; Mellot-Draznieks, C.; Bell, R. G. *J. Phys. Chem. C* **2009**, *113*, 544. (c) Sillar, K.; Hofmann, A.; Sauer, J. *J. Am. Chem. Soc.* **2009**, *131*(11), 4143.

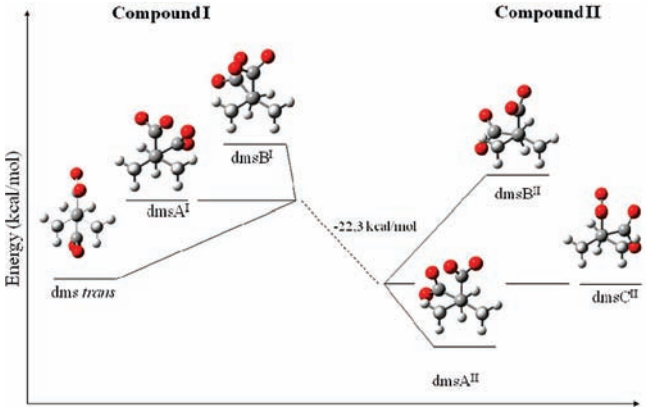

Figure 5. Relative energy scheme for dms conformers of compounds I and II.

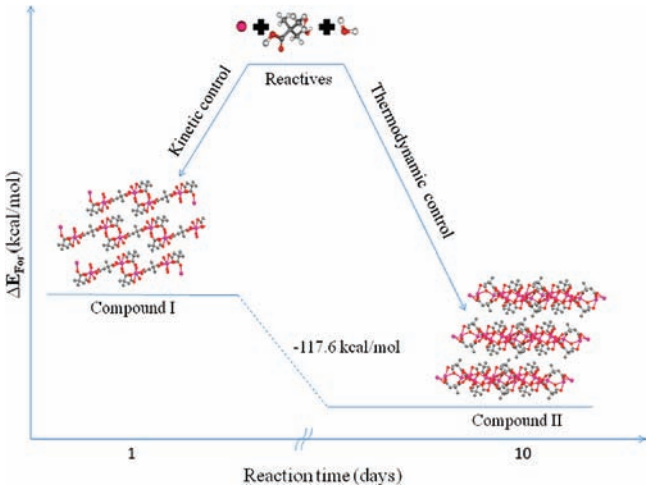

Figure 6. Relative formation energy for compounds I and II.

by X-ray diffraction, even though no symmetry constraints were imposed in this case. The corresponding results schematically represented in Figure 6, show that the compound II is more stable than the compound I for 5.1 eV, or 117.6 kcal/mol. It is worth mentioning that both theoretical procedures lead to the conclusion that the higher energetic synthesis conditions used for compound II favor the formation of this stable phase in terms of both the ligand conformations and the structure itself. These results point to a kinetically controlled formation for compound I and a thermodynamically governed process for compound II, in concordance to the depicted structural features, since the higher condensation of the SBU and the incremented dms/water ratio in the coordination sphere of compound II promote the formation of a more robust and stable framework.

Thermal Analysis. TGA and DTA curves for compound I and II are shown in Supporting Information, Figure S1. The continuous weight decay observed at relatively low temperatures in the TGA curves of both compounds is attributed to water absorbed and accounts for their hygroscopic character.

Compound I. Dehydration proceeds in one stage with a weight loss of 9.2% (calc. 8.6%) consistent with the removal of all water molecules. A relatively broad endothermic DTA peak at 185 °C is associated with this

Scheme 1. Oxidation of Methylphenylsulfide

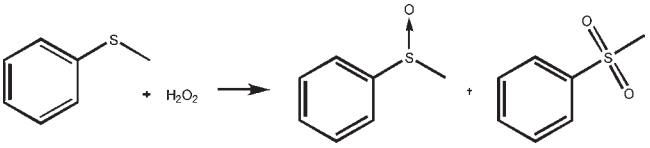

process. The second step is accompanied by a strong exothermic DTA signal at 410 °C and corresponds to the complete decomposition of the anhydrous compound. The calculated weight loss for the whole process (54.3%) is in a good agreement with the experimental value of 53.6%.

Compound II. A continuous weight loss of 3.4% is observed in the TGA curve between room temperature and ~265 °C, and it is associated with the elimination of the coordinated water molecule (calc. 2.3%). A practically negligible asymmetric endothermic signal is observed in the DTA curve at ~200 °C; this peak accounts for the dehydration process.

The second step in the TGA curve of II is denoted by a very intense exothermic DTA peak at 430 °C and corresponds to the complete decomposition of the dehydrated phase. The calculated and experimental weight losses for the whole process are in good agreement (calc. 51.2%, exp. 52.8%).

The final decomposition product for both compounds was identified as the cubic Er_2O_3 (PDF card 43−1007[34]).

Thermal Vibrational Study. The VT-FTIR spectra of compounds I and II are displayed in Supporting Information, Figures S2 and S4, respectively, where changes are marked with *. The fundamental vibrational modes of water molecules and carboxylate groups were assigned and are discussed briefly below.

Water Modes. A broad band can be observed in the OH stretching zone in the IR spectra of both compounds. The band shows several components consistent with the presence of water molecules that are involved not only in coordination to the metal ion but also in hydrogen bonds in the lattice. Two low-intensity bands located at 1678 and 1640 cm^{-1} are associated with the bending mode of coordinated water molecules of compound I, whereas several vibrational modes are observed in the 1000−600 cm^{-1} range. This fact, as well as the splitting of the bending mode, evidence the presence of differently involved water molecules in the lattice according to the structural model.

For compound II, most of the stretching modes of the water molecule appear slightly shifted to lower frequencies. No bending mode and only a few vibrational modes can be identified in the corresponding spectrum.

The bands located in the 300 cm^{-1} region are assigned to Er−Ow stretching mode since they are modified upon dehydration.

Carboxylate Groups Modes. The antisymmetric stretching vibrations appear as broad, asymmetric bands with various components included that can be explained in terms of the variety of coordination types exhibited by these groups. Splitting of the OCO stretching modes is not observed in the IR spectra of metal succinates, where only

(34) International Centre for Diffraction Data. JPCDS database. PDF-2 (**2003**).

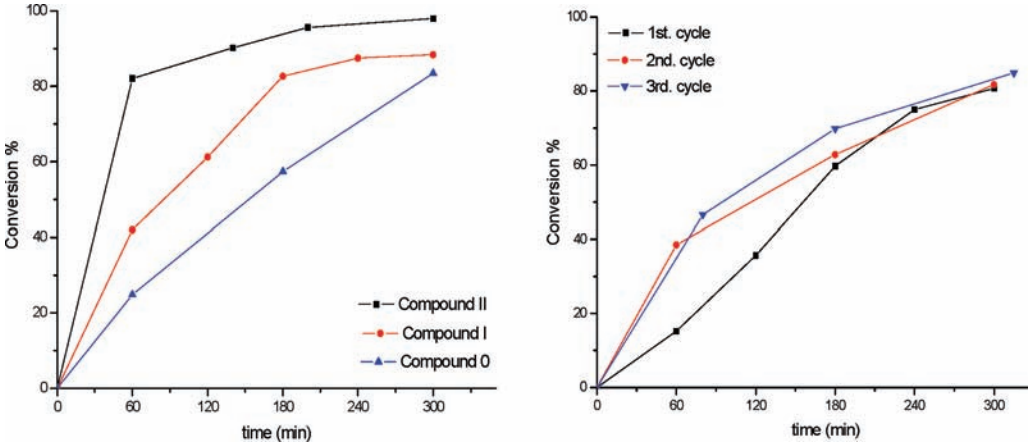

Figure 7. Kinetic profiles of oxidation of methylphenylsulfide with compounds 0, I, and II as catalysts (left); kinetic profiles in three consecutive reaction cycles employing compound I as catalyst (right).

one binding mode for carboxylate groups has been reported.[35]

It is worth noting that the additional component at higher frequency (1610 cm^{-1}) in the spectrum of compound II can be tentatively ascribed to the "malonate mode" derived from dms B^{II}. Several works dealing with metal malonate complexes that contain the six-membered ring originated in the mentioned mode, report this band as the spectroscopic evidence.[31a,36] Different ways of coordination do not seem to affect the symmetric OCO stretching vibration that appears without splitting at ~1400 cm^{-1}. The presence of dimethylsuccinic acid is discarded because no evidence of IR carbonyl absorption is present.

The bands located at ~400 cm^{-1} are asigned to Er−OCO strectching mode, which is consistent with the data reported in the literature for this vibration.[37]

Catalytic Activity Test: Oxidation of Methylsulfanylbenzene. Sulfoxides and other organosulfur compounds are important synthetic intermediates in organic chemistry[38] and are valuable in the preparation of biologically and pharmaceutically relevant materials.[39] For example, one of the oxidation reactions important in pharmaceutical research and production is that of a sulfide to a sulfoxide, which is achieved with a very wide variety of reagents.[40] Since sulfoxides can undergo overoxidation to sulfones, it is important that the catalyst has a suitable reactivity and converts selectively sulfides to sulfoxides. Continuing with our previous studies on the catalytic activity of rare earth succinates,[41,42] compounds I and II were tested as redox catalysts in the oxidation of methylphenylsulfide with H_2O_2 as the oxygen source (see Scheme 1). The results are summarized in Figure 7. In the case of compound I, the use of 1.5 equiv of H_2O_2 and its controlled addition allowed a significant improvement of the chemoselectivity of the process, and sulfoxide was obtained as the major product (selectivity = 84%). The obtained results demonstrate that compound I is an efficient catalyst and catalyzes selectively the sulfoxide formation under mild conditions, with a good yield (~65% after 4 h of reaction, TOF = 2118 h^{-1}). Compound II is more active (TOF = 4140 h^{-1}), but causes the overoxidation to the sulfone, showing a selectivity toward the sulfoxide of 47%.

To compare these catalytic behaviors with that of our previously reported Yb succinate framework (compound 0 from now on), we have performed the same reaction using it as catalyst in the new optimized conditions; the resulting TOF value is 1536 h^{-1} (457 h^{-1} under the previous condition,[42] 50% conversion in 6 h), with a conversion of 80% in 5 h. No induction period is observed under these new conditions, neither for Yb compound nor for the erbium-contained ones (Figure 7).

The two Er compounds (I and II) were found to be more active than that of Yb (compound 0). All compounds studied contain octa-coordinated lanthanide atoms, but the Er cation tends to get nine or even higher coordination number, which favors, from a mechanistic point of view, the intermediate species formation during the catalytic process.

Compound II, in which one half of the Er cations are coordinated to eight carboxylate oxygen atoms and the other half, to seven carboxylate oxygen atoms and one water molecule, is more active than compound I, where all Er atoms are coordinated to six carboxylate oxygen atoms and to two water molecules. From this fact we can infer that the Ln−O−OH intermediate specie is formed by increasing the lanthanide coordination number, and that no displacement of the water molecules takes place during the process. In short, activity decreases in the II > I > 0 direction, and as it is usual, selectivity decreases in opposite direction, 0 > I > II.

(35) (a) Brusau, E. V.; Pedregosa, J. C.; Echeverría, G.; Pozzi, G.; Punte, G.; Narda, G. E. *J. Coord. Chem.* **2001**, *54*, 469. (b) Kim, Y. J.; Jung, D.-Y. *Inorg. Chem.* **2000**, *39*, 1470.
(36) (a) Tapparo, A.; Heath, S.; Jordan, P.; Moore, G.; Powell, A. *J. Chem. Soc., Dalton Trans.* **1996**, 1601. (b) Brusau, E. V.; Pedregosa, J. C.; Narda, G. E. *J. Argent. Chem. Soc.* **2004**, *92*(1/3), 43.
(37) Ross, S. D. *Inorganic Infrared and Raman spectra*; McGraw-Hill Book Company: London, 1972.
(38) (a) Cremlyn, R. J. *An Introduction to Organosulfur Chemistry*; John Wiley & Sons: England, 1996; (b) Page, P. *Organosulfur Chemistry: Synthetic and Stereochemical Aspects*; Academic Press: Great Britain, 1998; Vol. *2*.
(39) (a) Carreño, M. C. *Chem. Rev.* **1995**, *95*, 1717. (b) Fernández, I.; Khiar, N. *Chem. Rev.* **2003**, *103*, 3651.
(40) Caron, S.; Dugger, R. W.; Ruggeri, S. G.; Ragan, J. A.; Brow Ripin, D. H. *Chem. Rev.* **2006**, *106*, 2943.
(41) Perles, J.; Iglesias, M.; Ruiz Valero, C.; Snejko, N. *J. Mater. Chem.* **2004**, *14*, 268.
(42) Bernini, M. C.; Gándara, F.; Iglesias, M.; Snejko, N.; Gutierrez-Puebla, E.; Brusau, E.; Narda, G. E.; Monge, M. A. *Chem.—Eur. J.* **2009**, *15*, 4896.

The only structural reason for the higher activity of compound II over compound I is the proximity of the metallic centers in the sharing edges/vertex polyhedron chains of the former, while the latter bears a more dispersed distribution of metallic catalytic centers. This difference might also be responsible for the low selectivity of the compound II.

Recycling Experiment. To investigate the lifetime and the stability of the better catalyst (compound I), a recycling experiment was performed employing it in three consecutive reaction cycles. As in the case of our previous study using an ytterbium succinate MOF,[42] the observed activity is kept over the three cycles of reaction, being slightly better in the third one (Figure 7-right). Induction periods were not observed in any cycle of reaction, which suggests the major activity of the new material in comparison with the ytterbium compound. This fact is also reflected in the bigger conversion values reached in a minor time.

The catalyst employed in the three consecutives cycles of reaction was separated by filtration, washed with diethyl ether, and then characterized by powder X-ray diffraction (PXRD) and IR spectroscopy. The comparison of the PXRD patterns of the catalyst before and after the recycling allows us to confirm that the crystalline structure of the compound is unaltered after the three cycles of reaction. On the other hand, in the IR spectrum of the catalyst one can observe the presence of two new bands (marked with * in Supporting Information, Figure S4) situated at ~530 and 505 cm^{-1} due probably to the existence of a Ln−O−OH intermediate, as it was found in a similar experiment on ytterbium succinate MOF.[42]

Conclusions

Two new compounds based on 2,2-dimethylsuccinate and Erbium(III) ion were obtained and completely characterized. By tuning the synthesis conditions, the two compounds were obtained as pure phases. Both compounds form polymeric two-dimensional structures, in which the Er cation is octacoordinated. It is highlighted as a design trend that the use of a gem-dimethylsubstituted aliphatic ligand along with a scanning of the synthesis conditions may increase the chances of obtaining frameworks with very different structural characteristics (such as a non-centrosymmetric or a centrosymmetric compound).

On the other hand, the employ of the two DFT calculation procedures show that the higher energetic synthesis conditions used for compound II favor the formation of this stable phase, which is reflected both in the ligand conformations as well as in the crystalline structure. These results indicate a kinetically controlled formation for compound I and a thermodynamically governed process for compound II, which agrees with the depicted structural features.

The new compounds exhibit activity as redox heterogeneous catalysts, compound I being the best one for the oxidation of methylphenylsulfide in comparison with compound II and with the previous Yb succinate MOF.[42]

Acknowledgment. This work has been supported by the Spanish MCYT Project Mat 2007-60822, MAT2006-14274-C02-02, and Consolider-Ingenio CSD2006−2001. Allocation of computational time on the CESCA supercomputer of the Centre de Supercomputació de Catalunya is acknowledged. G.E.N is a member of Consejo Nacional de Investigaciones Científicas y Técnicas (CONICET), and M.C.B. acknowledges a CONICET fellowship.

Supporting Information Available: Figures S1−S4 and Table S1. This material is available free of charge via the Internet at http://pubs.acs.org.